Control-oriented Linear Dynamic Wind Farm Flow and Operation Model

Jonas Kazda[1] and Nicolaos Antonio Cutululis[1]
[1]DTU Wind Energy
Correspondence: Jonas Kazda (kazd@dtu.dk)

Abstract.

The use of dynamic wind farm flow models can be beneficial for power reference following wind farm control. However, currently investigated flow models are nonlinear and can be computationally expensive, while many control approaches require linear models. This work therefore presents a newly developed wind farm operation modelling approach, the Dynamic Flow Predictor. The Dynamic Flow Predictor provides predictions of wind speed and turbine power using a computationally effective, linear, dynamic state space model. The model estimates wind turbine aerodynamic interaction using a linearized engineering wake model in combination with a delay process. Simulations of two turbines and eight turbines in SimWindFarm show that the Dynamic Flow Predictor can provide accurate estimates and predictions of wind turbine rotor effective wind speed and power. Nonetheless, the Dynamic Flow Predictor requires only 0.5% of the states of a dynamic two-dimensional computational fluid dynamics model used in wind farm control. The presented modelling approach is thus well suited for the use in wind farm control, while it is envisioned that the model can also be useful for wind turbine control and as a virtual wind turbine sensor.

1 Introduction

The turbulent nature of wind farm flow (Crespo and Hernández, 1996) drives the need for predicting wind speed dynamics at wind turbines in certain areas of wind farm control and wind turbine control. Therefore investigated prediction approaches for wind farm control and wind turbine control are individual turbine-focused prediction methods (Riverso et al., 2017; Mikkelsen et al., 2013; Schlipf et al., 2013) and wind farm-scale, dynamic flow models (Boersma et al., 2016; Soleimanzadeh et al., 2014). These prediction approaches differ in the targeted prediction horizon. Whereas individual turbine-focused prediction methods typically aim to predict up to 1min into the future, wind farm-scale flow models target prediction horizons in the order of time-scales of the aerodynamic interaction of wind turbines, that is horizons ranging between 1min and 10min.

Individual turbine-focused prediction approaches use turbine-based measurements or remote sensing in the turbine's proximity to predict the evolution of wind speed at that turbine. The turbine-based or remote sensing measurements are input to a predictor such as statistical models (Riverso et al., 2017; Knudsen et al., 2011) and / or machine learning (Wang and Hu, 2015). An overview of wind speed prediction methods can be found in Jung and Broadwater (2014). Individual turbine-focused prediction methods do, however, not consider the effect of wind turbine operation on the aerodynamic interaction of wind turbines. The aerodynamic interaction of wind turbines is explicitly modelled in wind farm-scale flow models.

The modelling of aerodynamic interaction effects is beneficial in certain areas of wind farm control. In wind farm control the operation of the whole wind farm is optimized by using a coordinated control algorithm that specifies the operation point of each turbine. Common objectives in wind farm control either aim to (i) maximise the total power of the wind farm or (ii) follow a specified reference for the total power of the wind farm. Some approaches perform a multi-objective optimization that simultaneously also aims to reduce the fatigue loads of wind turbines. In approaches with the former objective, that is the maximisation of the total power, static wind farm-scale flow models (Gebraad et al., 2016; Kazda et al., 2016a) are typically used to model the aerodynamic interaction of wind turbines. In control approaches with the latter objective, that is to follow a reference for the total power of the wind farm, wind farm flow model-based approaches are investigated in recent research. Shapiro et al. (2018) showed that the use of dynamic flow models can be beneficial as compared to the use of static models. The dynamics included in the investigated dynamic flow model are transport delays in wake dynamics. The time scale of these dynamics are of similar magnitude as the time scale of certain type total power reference signals used in wind farm control. Shapiro et al. (2018) argue that the use of a dynamic flow model is therefore more beneficial.

A variety of dynamic models are investigated in literature for the use in wind farm control. These models are based on either engineering wake models (Gebraad and van Wingerden, 2014; Göçmen et al., 2016; Shapiro et al., 2018) or two-dimensional computational fluid dynamics (CFD) (Boersma et al., 2018; Soleimanzadeh et al., 2014). The latter models, that are two-dimensional CFD approaches, estimate hub height wind farm flow using customized, two-dimensional Navier-Stokes equations. The value proposition of such models is that wind farm flow is not only estimated at turbine locations, but in the entire hub height plane of the wind farm. The use of a CFD model is, however, typically more computationally expensive than the use of engineering models. Engineering models are used in the formerly mentioned models of wind farm flow. Some of these models have been used in nonlinear model predictive controllers for optimizing wind farm operation. However, running the optimization is currently in the order of minutes (Shapiro et al., 2018). In order to reduce the duration of the optimization, linear model predictive control can be employed. Such approach, however, requires a linear, dynamic model.

Therefore, we developed a dynamic, linear wind farm flow and operation model, the Dynamic Flow Predictor. The model estimates the aerodynamic interaction of wind turbines using a linearized engineering wake model in combination with a delay process. The aim is that the linear nature of the model and the use of an engineering wake model results in low computational cost.

The structure of the article is as follows. In Section 2, the methodology is detailed. In Section 3, the performance of the model is discussed in two case studies. The paper concludes with a summary of the key findings in Section 4.

2 Methods

The newly developed Dynamic Flow Predictor and the simulation environment used for testing the model are described in the following.

2.1 Dynamic Flow Predictor

The developed Dynamic Flow Predictor is a linear, dynamic, discrete time wind farm operation model. Figure 1 shows the model's system structure, which consists of a flow model and a turbine power model, which are introduced in the following.

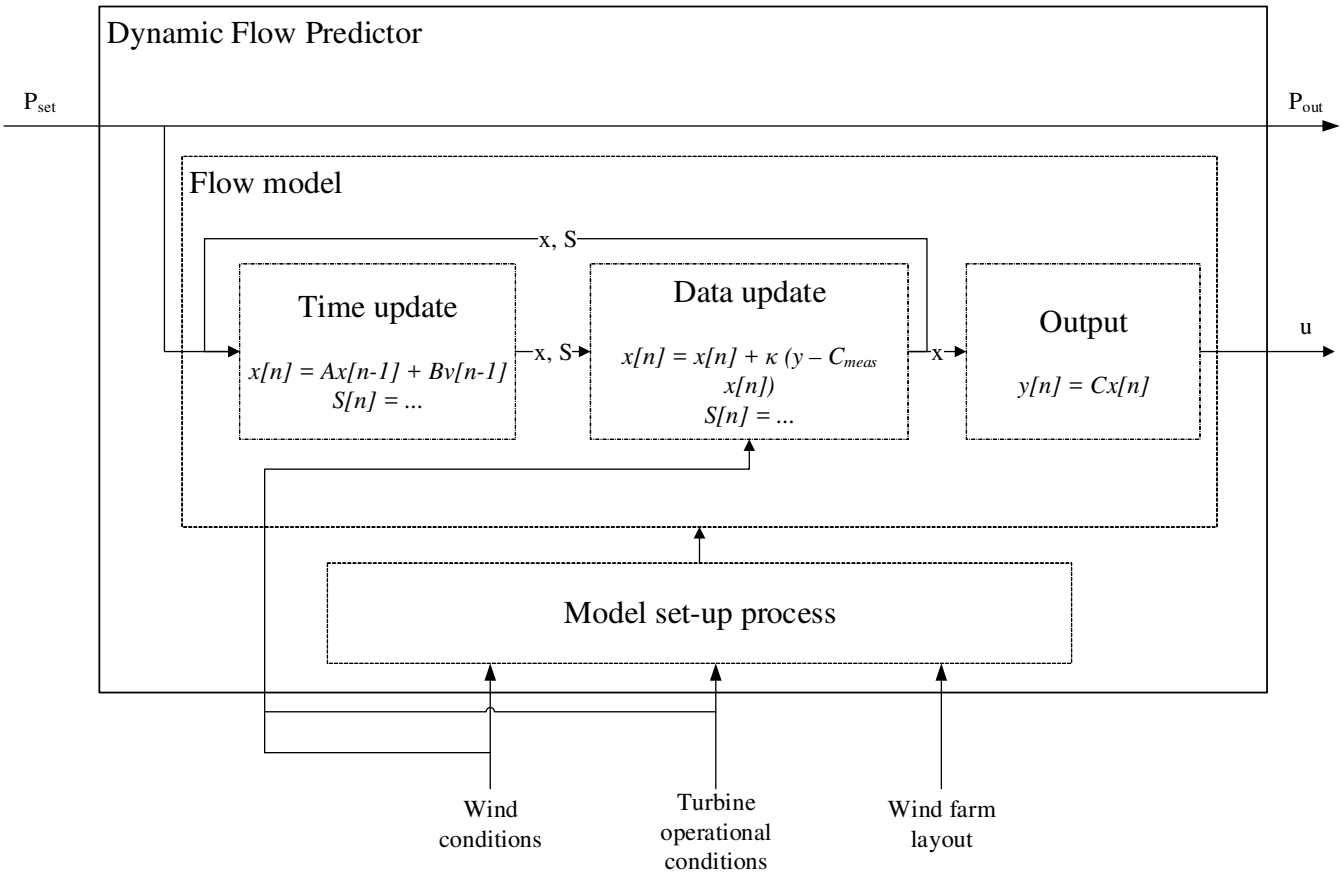

Figure 1. System structure of Dynamic Flow Predictor showing system update process and Kalman filter time update and data update.

2.1.1 Turbine operation model

As shown in Figure 1, turbine power P is modelled using a direct feed-through. As such the modelled turbine power output P_{out} equals the turbine power set-point P_{set} as

$$P = P_{set} = P_{out} \tag{1}$$

This assumption is valid if relevant turbine dynamics are either much faster or much slower than the sampling time. The sampling time used in the present work is 30s. The relevant, in this case, fast turbine dynamics are generator power dynamics

and blade pitch control dynamics, which are typically in the order of seconds. It is thus assumed that the dynamics of turbine power production can be modelled using algebraic variables.

2.1.2 Flow model

The flow model consists of a set of modules, where each module accounts for the interaction of one or multiple upstream turbines and a single downstream turbine. These interaction models are joined together to a total flow model according to the overall aerodynamic interaction of the wind turbines in the wind farm. The aerodynamic interaction of one or multiple upstream turbines with a downstream turbine is modelled as

$$u_i[n] = u_\infty[n - \kappa_\infty] - \sum_{l=1}^{L_i} \delta\tilde{u}_{i,l}[n - \kappa_{i,l}] \tag{2}$$

where u_i is the rotor effective wind speed of downstream turbine *i* at discrete time *n*. The rotor effective wind speed is the wind speed in the mean wind direction averaged over the rotor area of a wind turbine. All wind speeds in the present work are rotor effective wind speeds. u_∞ is the wind speed at the most upstream turbine and $\delta\tilde{u}_{i,l}$ is the wake deficit induced from upstream turbine *l* to downstream turbine *i*. L_i is the number of turbines upstream of turbine *i*. κ_∞ is the discrete time delay of the wake from the most upstream turbine to propagate to downstream turbine *i*. $\kappa_{i,l}$ is the discrete time delay of the wake from upstream turbine *l* to propagate to downstream turbine *i*. The discrete time delay κ is defined as the integer-rounded ratio of the wake propagation delay δt and the sampling time T_s as $\kappa = (\delta t/T_s)_{round}$.

The duration of wake propagation δt is determined using an engineering model (Machefaux et al., 2015). The aim is to choose the model that matches the considered wind farm as close as possible. In SimWindFarm the wake propagation speed is proportional to freestream flow. Thus, the model for the wake propagation delay δt is chosen for this work to be calculated as $\delta t = \delta x/u$, where u is the measured wind speed and δx the distance of the propagated wake.

The wake deficit is modelled based on the Frandsen wake model (Frandsen et al., 2006), which estimates the wake deficit $\delta u_{i,l}$ as

$$\delta u_{i,l}(P_l, u_l) = \frac{1}{2} c_T(P_l, u_l)\Big(1 + \frac{\delta x}{4R_l}\Big)^{-1} u_l \frac{A_{overlap,l,i}}{A_{rotor,i}} \tag{3}$$

where c_T is the thrust coefficient of turbine l, P_l is the turbine's power and δx the distance from turbine l to turbine i in the mean wind flow direction. R_l is the radius of the rotor of the upstream turbine, $A_{overlap,l,i}$ is the overlap area of the wake from upstream turbine l with the rotor area of downstream turbine i. $A_{rotor,i}$ is the rotor area of downstream turbine i.

The Frandsen model is chosen as the same wake deficit model is used in the simulation environment, but other wake models can be used similarly. Given the multitude of wake deficit models available in literature, the aim is generally to choose the

model that matches the considered wind farm as close as possible. The linearized wake deficit, as used in Eq. 2, is modelled using the 1^{st} order Taylor series expansion of the wake deficit model as

$$\delta\tilde{u}_{i,l} = \delta u_{i,l,0} + \frac{\partial \delta u_{i,l}}{\partial u_l}\Big|_{x_0} \Delta u_l + \frac{\partial \delta u_{i,l}}{\partial P_l}\Big|_{x_0} \Delta P_l \tag{4}$$

where Δu_l is the deviation of u_l from the wind speed linearization point $u_{l,0}$, ΔP_l denotes the deviation of turbine power P_l from the power linearization point $P_{l,0}$, and x_0 is the overall system linearization point. The partial derivatives of the Frandsen wake deficit model with respect to wind speed and turbine power are

$$\frac{\partial \delta u_{i,l}}{\partial u_l}\Big|_{x_0} = \frac{1}{2}\Big(1+\frac{\delta x}{4R_l}\Big)^{-1} \frac{A_{overlap,l,i}}{A_{rotor,i}} \Big(c_T(P_{l,0},u_{l,0}) + u_l \frac{\partial \delta c_{T,l}}{\partial u_l}\Big|_{x_0}\Big) \tag{5}$$

$$\frac{\partial \delta u_{i,l}}{\partial P_l}\Big|_{x_0} = \frac{1}{2}\Big(1+\frac{\delta x}{4R_l}\Big)^{-1} \frac{A_{overlap,l,i}}{A_{rotor,i}} u_l \frac{\partial \delta c_{T,l}}{\partial P_l}\Big|_{x_0} \tag{6}$$

The partial derivates of the wake deficit model (Eq. 5 and Eq. 6) are used in the linearized wake deficit model (Eq. 4), which is employed in the wake superposition model (Eq. 2). After converting the wake superposition model to state space form and joining all wake interaction processes, the total wind farm flow model can be written as

$$\underbrace{\begin{bmatrix} \boldsymbol{u}_{del,all} \\ \boldsymbol{u}_0 \end{bmatrix}}_{\boldsymbol{x}}[n+1] = \underbrace{\begin{bmatrix} \mathbf{A}_{del,all} + \mathbf{B}_{u,all}\mathbf{C}_u & \mathbf{B}_{u_0,all} \\ 0 & \mathbf{I} \end{bmatrix}}_{\mathbf{A}} \underbrace{\begin{bmatrix} \boldsymbol{u}_{del,all} \\ \boldsymbol{u}_0 \end{bmatrix}}_{\boldsymbol{x}}[n] + \underbrace{\begin{bmatrix} \mathbf{B}_{\Delta P,all} \\ 0 \end{bmatrix}}_{\mathbf{B}} \underbrace{\Delta \boldsymbol{P}[n]}_{\boldsymbol{v}} \tag{7}$$

$$\boldsymbol{u}[n] = \underbrace{\begin{bmatrix} \mathbf{C}_u & 0 \end{bmatrix}}_{\mathbf{C}_{u,tot}} \underbrace{\begin{bmatrix} \boldsymbol{u}_{del,all} \\ \boldsymbol{u}_0 \end{bmatrix}}_{\boldsymbol{x}}[n] \tag{8}$$

$\boldsymbol{u}_{del,all}$ is the wind speed delay states of all wind turbines, $\boldsymbol{u}_0$ is the wind speed linearization point. Output of the flow model is the current rotor effective wind speed $\boldsymbol{u}$ at the turbines in the wind farm. $\Delta \boldsymbol{P}$ is the deviation of the turbine power set-points from the power linearization point. Matrix $\mathbf{A}_{del,all}$ models the process of wake propagation delay of all turbines and matrices $\mathbf{B}_{u,all}$, $\mathbf{B}_{u_0,all}$ and $\mathbf{B}_{\Delta P,all}$ model the effect of wake deficit on wind flow. Matrix $\mathbf{C}_u$ relates the wind speed states $\boldsymbol{u}_{del,all}$ to the current rotor effective wind speed $\boldsymbol{u}$ at the turbines in the wind farm.

In the following the total system state space model as presented in Eq. (7) is summarized as

$$\boldsymbol{x}[n+1] = \mathbf{A}\boldsymbol{x}[n] + \mathbf{B}\boldsymbol{v}[n] \tag{9}$$

$$\boldsymbol{u}[n] = \mathbf{C}_{u,tot}\boldsymbol{x}[n] \tag{10}$$

where $\boldsymbol{x}$ is the state vector and $\boldsymbol{v}$ is the control input vector. $\mathbf{A}$ and $\mathbf{B}$ are system process matrices and $\mathbf{C}_{u,tot}$ is the wind speed output matrix.

2.2 Kalman filter and system update

The model update process is structured into three steps: (1) Time update, (2) data update and (3) system matrix update. The first two steps constitute an ordinary Kalman filter (Kalman and Bucy, 1961). The Kalman filter is used to improve the prediction accuracy of the Dynamic Flow Predictor, by correcting the states of the flow model. A Kalman filter is chosen as it allows correcting, as shown in the results section, the system states using a weighted average of measurements of selected states, with more weight given to measurements with larger certainty.

2.2.1 Time update

First, in the time update of the Kalman filter the state estimate from the prior time step $n-1$ is used to predict the current system state at time step n based on the system model of time step $n-1$. The time update is calculated as

$$\hat{\boldsymbol{x}}|_{n-1}[n] = \mathbf{A}|_{n-1}\hat{\boldsymbol{x}}|_{n-1}[n-1] + \mathbf{B}|_{n-1}\boldsymbol{v}[n-1] \tag{11}$$

where $\hat{\boldsymbol{x}}|_{n-1}$ is the state estimate condition to measurements up to time step $n-1$. Similarly, $\mathbf{A}|_{n-1}$ and $\mathbf{B}|_{n-1}$ are system matrices at time step $n-1$. The variance of the state estimate, $\mathbf{S}$, is updated as

$$\mathbf{S}|_{n-1}[n] = \mathbf{A}|_{n-1}\mathbf{S}|_{n-1}[n-1]\mathbf{A}^T|_{n-1} + \mathbf{R}_1|_{n-1} \tag{12}$$

where $\mathbf{R}_1$ is the covariance of the process error. The covariance is estimated using physics-based estimates of the model errors.

2.2.2 Data update

Second, in the data update of the Kalman filter the system state is updated with present system measurements, that are related to system states as

$$\hat{\boldsymbol{y}}_{meas}[n] = \mathbf{C}_{meas}|_{n-1}\hat{\boldsymbol{x}}[n] \tag{13}$$

The measurements $\hat{\boldsymbol{y}}_{meas}$ are wind speeds related to selected wind speed states of the flow model, such as the current rotor effective wind speed at wind turbines. Matrix $\mathbf{C}_{meas}$ relates the system states to these measurements.

The Kalman gain κ is calculated as

$$\kappa|_n = \mathbf{S}|_{n-1}[n]\mathbf{C}_{meas}^T|_{n-1}(\mathbf{C}_{meas}|_{n-1}\mathbf{S}|_{n-1}[n]\mathbf{C}_{meas}^T|_{n-1} + \mathbf{R}_2|_{n-1})^{-1} \tag{14}$$

where $\mathbf{R}_2$ is the covariance of the measurement noise. The covariance is estimated using physics-based and empirical estimates of the measurement errors. The cross-correlation between $\mathbf{R}_1$ and $\mathbf{R}_2$ is modelled to be zero. The data update is performed as

$$\hat{\boldsymbol{x}}|_n[n] = \hat{\boldsymbol{x}}|_{n-1}[n] + \kappa|_n(\boldsymbol{y}_{meas}[n] - \mathbf{C}_{meas}|_{n-1}\hat{\boldsymbol{x}}|_{n-1}[n]) \tag{15}$$

$$\mathbf{S}|_n[n] = \mathbf{S}|_{n-1}[n] - \mathbf{S}|_{n-1}[n]\mathbf{C}^T_{meas}|_{n-1}(\mathbf{C}_{meas}|_{n-1}\mathbf{S}|_{n-1}[n]\mathbf{C}^T_{meas}|_{n-1} + \mathbf{R}_2|_{n-1})^{-1}\mathbf{C}_{meas}|_{n-1}\mathbf{S}|_{n-1}[n] \tag{16}$$

2.2.3 Matrix update

Third, system matrices are updated based on the current system operation point. The update approach depends on the deviation of the current system state from the linearization point. If the deviation exceeds the update limit ϵ_{upd} the system matrices are updated and as a result the new linearization point equals the current system state. If the deviation is within the limits the system matrices remain unchanged. Consequently, a matrix update is performed if the following condition is satisfied.

$$\epsilon_{upd} < \frac{|x - x_0|}{x_0} \tag{17}$$

where ϵ_{upd} is the update limit, which is set to 0.25 in this work. The choice of the update limit is a trade-off between model accuracy and computational efforts. More details in this regard are discussed in section 3.1.4. x represents a relevant system condition such as wind conditions and turbine operation point, and x_0 the linearization point of that condition.

2.3 SimWindFarm simulation environment

The Dynamic Flow Predictor is tested in simulations using the dynamic simulation framework SimWindFarm (Grunnet et al., 2010, 2016). SimWindFarm performs simultaneous, dynamic simulations of the wind turbines in the wind farm, the wind farm control, the aerodynamic interaction of the wind turbines and the actions by the transmission system operator. The NREL5MW virtual turbine model (Jonkman et al., 2009) is used to model wind turbine operation. Wind turbine aerodynamics are modelled using the turbine power coefficient and thrust coefficient. Up to 3rd order dynamic models are employed to simulate the drive train, generator and pitch actuator. The aerodynamic model of the wind flow in the wind farm is structured into an ambient field model and a turbine wake model part. The ambient wind field is modelled as the hub height, turbulent wind flow advected with the mean wind speed under the assumption of Taylor's frozen turbulence. Wake flow modelling includes wake wind speed deficit, wake width expansion, wake meandering and wake merging. Wind turbines are controlled using the DTU Wind Farm Controller (Kazda et al., 2016b), which is linked to the SimWindFarm simulation tool and replaces the basic, standard wind farm controller in SimWindFarm.

All simulations use the same wind conditions, as shown in Table 1. The simulated wind conditions have a mean wind speed of 8m/s, a turbulence intensity of 6%. The wind direction is considered aligned with the turbine row, if not indicated differently in the discussion. The turbine arrays are spaced by 4.3 rotor diameters (D).

Table 1. Key characteristics of wind conditions used in all SimWindFarm simulations.

Mean wind speed	Turbulence intensity	Wind direction
8 m/s	6%	constant

3 Results & Discussion

The performance of the Dynamic Flow Predictor is assessed in a two turbine and an eight turbine case study. The aim of the two turbine case study is to showcase the performance, robustness and validity of the modelling approach. In the eight turbine case study, the model's performance is analyzed with respect to the model's application in wind farms.

3.1 Two turbine case study

In the following, first, the simulation set-up is introduced, second, the simulated wind farm operation scenario is presented, and third, the performance, robustness and validity of the model is discussed with respect to Kalman filtering, model update and wind direction.

3.1.1 Simulation set-up

The case study is performed in the dynamic simulation tool SimWindFarm. The layout of the simulated two turbine array is shown in Figure 2. As such turbine No. 1 is the upstream turbine and turbine No. 2 the downstream turbine.

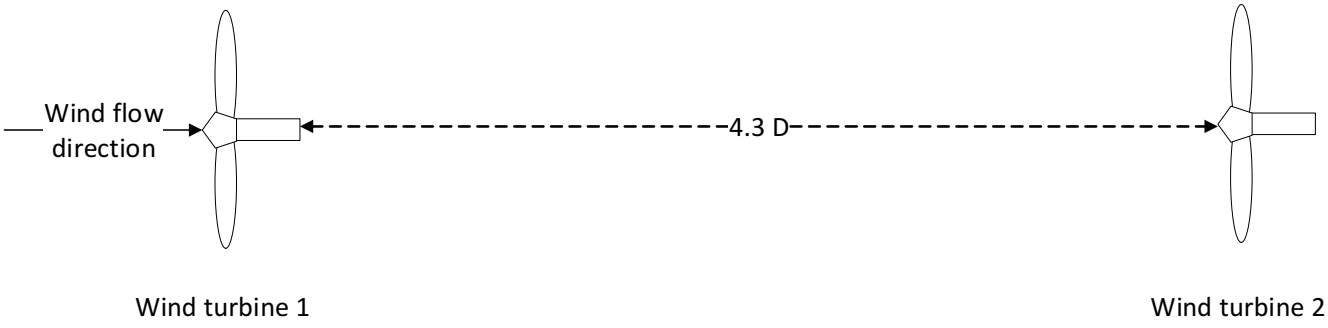

Figure 2. Layout of two turbine array used for test of Dynamic Flow Predictor.

3.1.2 Wind farm operation

The present design of the Dynamic Flow Predictor targets the prediction of wind farm flow and operation with the objective to follow a total power reference signal. The model tests are thus conducted in power reference following operation in both case studies. Both case studies use the same normalized total power reference signal, which represents the signal used in the wind farm ancillary service "balance control". The total power reference signal is further chosen as such that the resulting individual turbine power references never exceed a turbine's available power in any of both case studies. The limiting turbine in terms

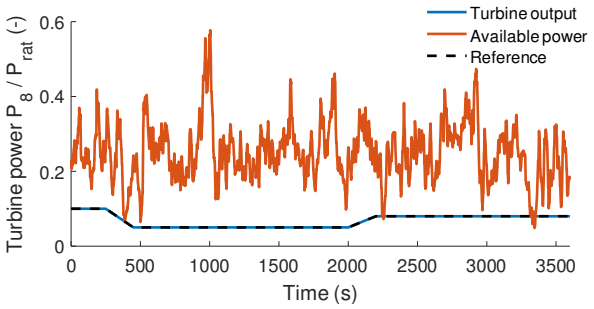

Figure 3. Simulated power output of most downstream turbine No. 8 of eight turbine array.

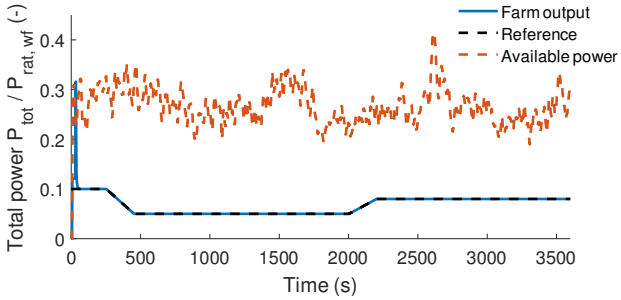

Figure 4. Simulated operation of two turbine array used for comparison with Dynamic Flow Predictor. Shown are (a) total farm power and (b) blade pitch angle.

of available power is the most downstream turbine of the eight turbine array of the eight turbine case study, as can be seen in Figure 3.

Figure 4.a shows the simulated total farm power output, the total power reference signal and the wind farm available power for the two turbine case study. The power is normalized with the rated wind farm power. The wind farm is controlled using the DTU Wind Farm Controller's closed-loop PI-controller with the equal dispatch function (Kazda et al., 2018) in both case studies. It can be observed, that the total farm power follows the total power reference well. The normalized root-mean-square deviation from the reference is 0.35%. The wind turbines are controlled using a standard wind turbine control approach (Pao and Johnson, 2009). The reduction of the turbines' power below the available power results in the turbines operating at the rated rotor rotational speed, while controlling aerodynamic power using the pitch controller. Figure 4.b. shows the simulated dynamics of the blade pitch angle of the wind turbines. The observed variation of the pitch angle results in a variation of the turbine's thrust and consequently, also in a variation of the wake deficit generated by that turbine.

3.1.3 Benefits of Kalman filtering

In Figure 5 the time series of wind speed is compared between the Dynamic Flow Predictor and SimWindFarm. Figure 5.a shows the wind speed at upstream turbine No. 1. It can be observed that the wind speed prediction by the Dynamic Flow

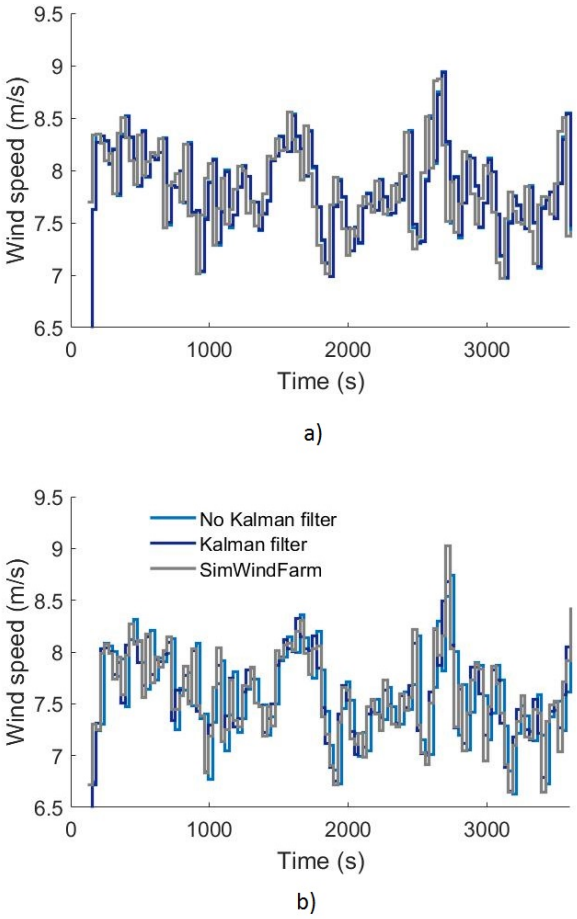

Figure 5. Sampled rotor effective wind speed simulated using SimWindFarm and predicted using Dynamic Flow Predictor with and without use of Kalman filter. Shown are wind speeds of (a) turbine No. 1 and (b) turbine No. 2.

Predictor is in good agreement with SimWindFarm. The normalized root-mean-square (RMS) deviation of the wind speed prediction of the Dynamic Flow Predictor is 4.8% both with and without the use of the Kalman filter. It is evident that there is a time lag of one time step in the wind speed estimates of the Dynamic Flow Predictor both with and without the use of the Kalman filter. This is due to the definition of the wind speed state in the Dynamic Flow Predictor. The wind speed state at a time step n is defined as the mean wind speed over the time interval $[nT_s, (n+1)T_s]$. The wind speed at the upstream turbine at time step n is calculated using a persistence-based prediction from the wind speed measurements over the time interval $[(n-1)T_s, nT_s]$. As a result, the Dynamic Flow Predictor wind speed estimate at the upstream turbine has a lag of one time step.

Figure 5.b shows the wind speed at downstream turbine No. 2. It can be observed that the Dynamic Flow Predictor predictions of wind speed are in good agreement with SimWindFarm. The normalized RMS prediction error is 4.4% without the use of the

Kalman filter. The use of the Kalman filter reduces the error by 70% to a RMS error of only 1.3%, as shown in Figure 6. The main benefit of using the Kalman filter is that the one step time lag propagating from the upstream turbine is removed and the wake deficit estimation is improved.

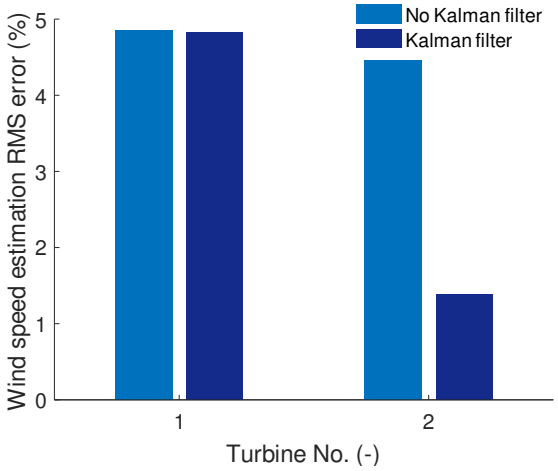

Figure 6. RMS deviation of rotor effective wind speed estimation at turbines of two turbine array. RMS deviation is normalised with mean freestream wind speed.

3.1.4 Model update frequency

In the following, we show that the Dynamic Flow Predictor's linearization approach is robust, so model matrix updates are required only seldom. The study is performed in the same wind conditions and wind farm operation as presented in section 3.1.2. The robustness of the linear model is thus tested in varying wind conditions and changing turbine operational settings. Figure 7 shows the sensitivity of the wind speed estimation accuracy and the model update frequency with respect to the update limit ϵ_{upd}. The estimation accuracy is the RMS error of rotor effective wind speed at downstream turbine No. 2. The wind speed estimation error at the upstream turbine is not part of this analysis, since it is not dependent on the matrix update. The update frequency is defined as the average ratio of matrix updates n_{upd} to model iterations n_{iter}. The study is performed without the use of the Kalman filter, so the estimation accuracy is only dependent on the linearization approach.

It can be observed that the linearization approach in the Dynamic Flow Predictor is robust. At least up to an update limit of 0.5 the wind speed prediction accuracy is insensitive to the update limit. An update limit of 0.5 is, for example, a 50% deviation of wind speed from the wind speed linearisation point. By increasing the update limit from 0.01 to 0.5, the update frequency decreases from 100% to 3%. Thus, the update frequency can be reduced by 97%, while estimating wind speed at the same accuracy. The 97% reduction in the update frequency results in an increased computational effectiveness of the Dynamic Flow Predictor.

It is further estimated that the Dynamic Flow Predictor requires only 0.5% of the states of a comparable, dynamic 2D CFD model. The state space system of the Dynamic Flow Predictor used for the two turbine case study has 5 states. A similar

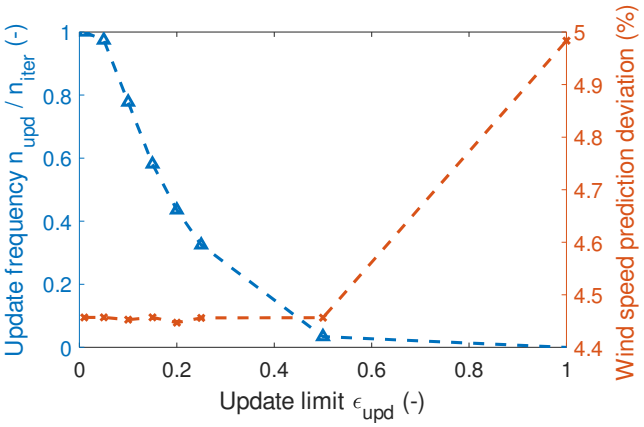

Figure 7. Impact of matrix update limit on downstream turbine wind speed prediction accuracy (right) and matrix update frequency (left).

two turbine set-up simulated using a 2D CFD model in (Doekemeijer et al., 2016) uses 1034 states. Both, the Dynamic Flow Predictor and mentioned 2D CFD model use sparse system matrices. Hence, the smaller number of states used in the Dynamic Flow Predictor can result in larger computational effectiveness.

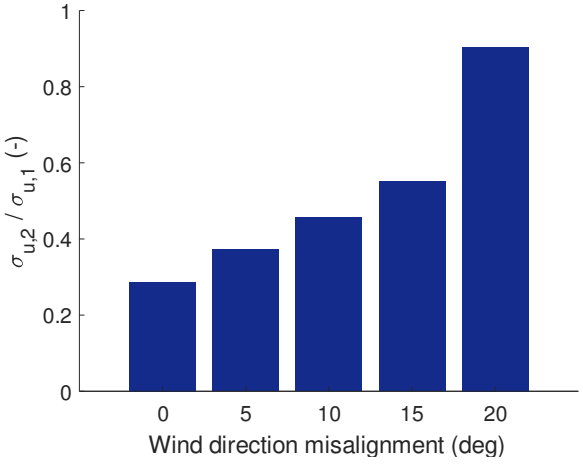

Figure 8. Effect of alignment of turbine array with wind direction on rotor effective wind speed estimation accuracy. Estimation accuracy is ratio of RMS wind speed estimation error at downstream turbine to RMS wind speed estimation error at upstream turbine.

3.1.5 Effect of wind direction

The following study shows that the model is suited for the full range of wind directions and wake situations in SimWindFarm. The Dynamic Flow Predictor's accuracy of wind speed prediction is, however, dependent on the alignment of the turbine array with the mean wind direction. Figure 8 shows the effect of the misalignment of the two turbine array with the wind direction

on the wind speed estimation accuracy at the downstream turbine. The study is performed with the use of the Kalman filter. The estimation accuracy is the RMS deviation of the Dynamic Flow Predictor wind speed prediction to the SimWindFarm flow model. The prediction accuracy of the downstream turbine is normalized with the prediction accuracy at the upstream turbine. The normalization is performed, since a different seed of the wind velocity field is used in each simulated wind direction. The simulations show a larger prediction error with an increase in misalignment. With larger misalignment, the correlation of the two turbines' wind speed decreases and thus results in an increasing error of the model. Nonetheless, the error at the downstream turbine is smaller than the persistence-based prediction error at the upstream turbine. At 20° misalignment the wake from the upstream turbine is not affecting the downstream turbine. Hence, the wind speed estimate at turbine No. 2 is also a persistence-based wind speed estimate. Since both turbines use persistence-based estimates, the ensemble average of the wind speed estimation error is expected to be the same at both turbines. The observed higher prediction accuracy at the downstream turbine is likely to be due to the seed of the turbulent wind field in SimWindFarm.

3.2 Eight turbine case study

In the eight turbine case study, the performance of the Dynamic Flow Predictor is demonstrated in key areas relevant to the model's application to large wind farms. Given the model's application areas, that is wind farm control, turbine control, and as virtual sensor, the model's performance is analyzed with respect to its accuracy in the prediction of wind speed and available turbine power. An eight turbine array is chosen for the analysis, as it resembles flow interactions present in large wind farms, which can typically be split into rows of turbines, such as the eight turbine array in the present work that is depicted in Figure 9.

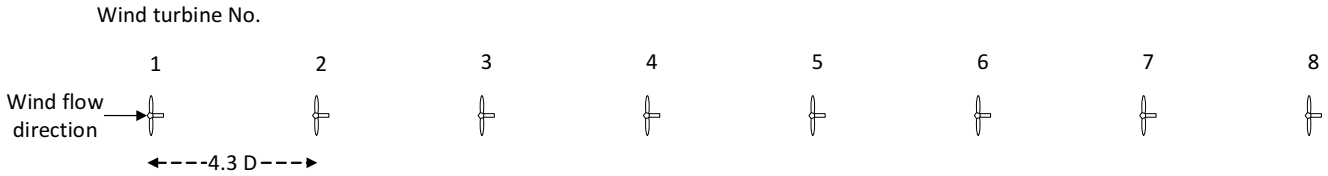

Figure 9. Layout of eight turbine array used for test of Dynamic Flow Predictor.

3.2.1 Wind speed estimation

Figure 10 shows the accuracy of the Dynamic Flow Predictor in estimating the rotor effective wind speed of the turbines of the eight turbine array. Reference to the Dynamic Flow Predictor is the SimWindFarm model. The accuracy is quantified as the RMS deviation of the The model prodives estimates of the rotor effective wind speed averaged over a horizon of As in the two turbine case study, it is observed that the use of the Kalman filter improves the estimation accuracy. The average improvement is 70%. Without the use of the Kalman filter, the estimation error tends to increase with downstream turbines. This is due to the accumulation of the estimation error with downstream turbines. With the use of the Kalman filter the estimation error ranges from 0.6% to 3.5% at downstream turbines. The wind speed estimated using the Dynamic Flow Predictor can be used in wind

farm control, wind turbine control and as virtual wind speed sensor of wind turbines. For the use as virtual sensor the wind speed estimate could substitute missing or erroneous sensors on wind turbines. Alternatively, the wind speed estimate could be used as reference to existing wind speed measurements at a wind turbine.

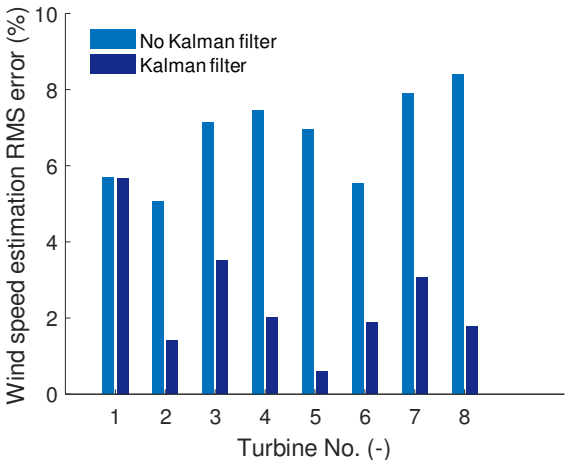

Figure 10. Statistics of normalized root-mean square error in estimation of current rotor effective wind speed at turbines of eight turbine array.

3.2.2 Wind speed prediction

The analysis of the model's capability for future wind speed prediction shows that the Dynamic Flow Predictor can provide wind speed predictions with an error of less than 4% over a time horizon of up to 5min as compared to SimWindFarm in this case study. Figure 11 and Figure 12 show the accuracy of the ten-step-ahead prediction of wind speed at the turbines of the eight turbine array. Wind speed predictions are calculated using the state space-driven prediction approach employed in model predictive control. The accuracy is quantified using the RMS difference between the Dynamic Flow Predictor predictions and SimWindFarm. The results shown in Figure 11 are obtained without the use of the Kalman filter. It can be observed that at the downstream turbines the prediction error is close to constant over several prediction steps and then jumps to a higher level of prediction error. This can be seen, for example, in Figure 12 at turbine No. 5 from prediction step 8 to prediction step 9. The number of steps with close to constant prediction accuracy equals to the number of the model's internal delay states. Further downstream turbines have a longer accurate prediction horizon due to the larger number of internal delay states. Predictions beyond the model's internal delay states are based on persistence and thus less accurate. Future work aims to extend the length of the accurate prediction horizon by exchanging the persistence-based wind speed estimate at the upstream turbine with an individual turbine-focused prediction method such as a statistical model as used in (Riverso et al., 2017).

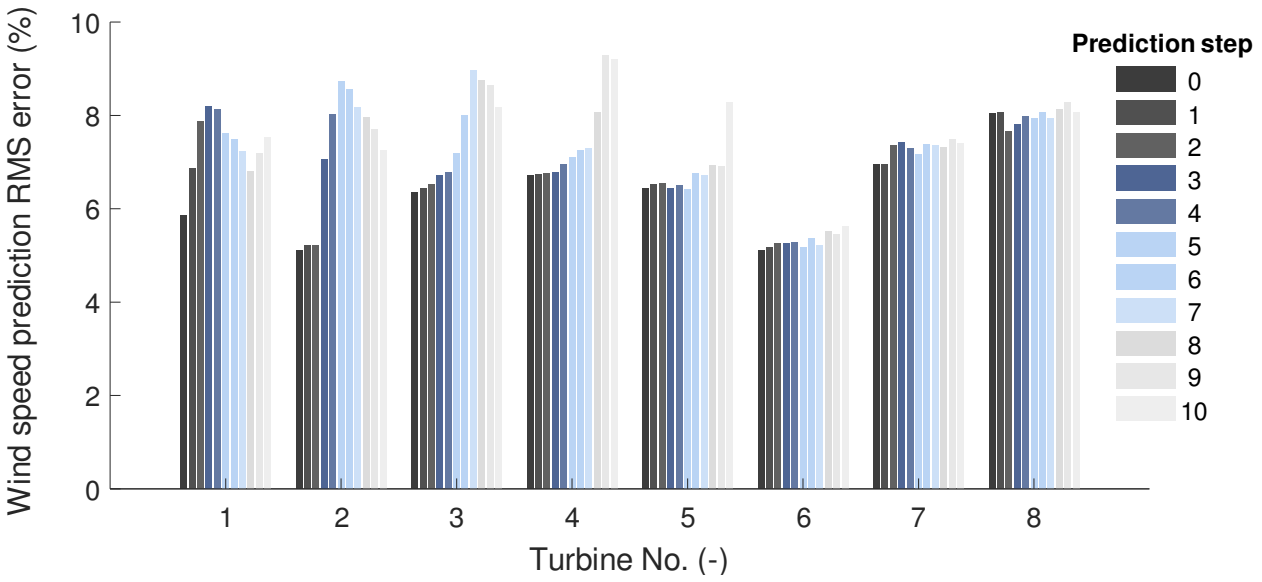

Figure 11. RMS error of 10-step ahead prediction of rotor effective wind speed at turbines of eight turbine array. Prediction is performed by Dynamic Flow Predictor without use of Kalman filter.

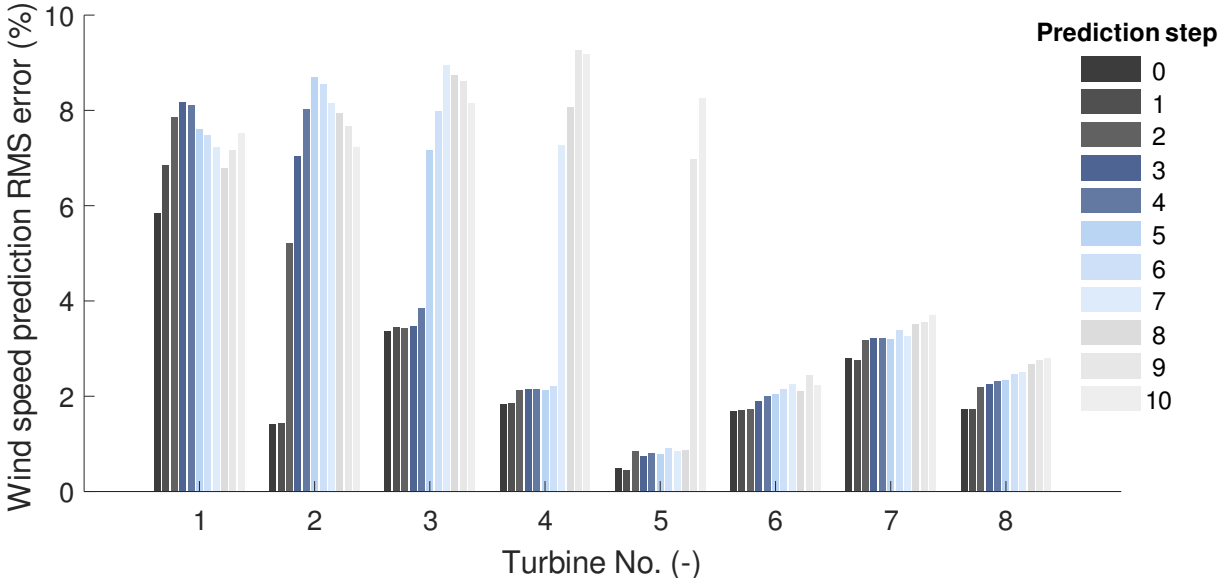

Figure 12. RMS error of 10-step ahead prediction of rotor effective wind speed at turbines of eight turbine array. Prediction is performed by Dynamic Flow Predictor with use of Kalman filter.

The results in Figure 12 show the same predictions, but obtained with the use of the Kalman filter. The prediction accuracy is improved in the prediction steps, which are based on the model's internal delay states, as compared to the results generated without the use of the Kalman filter. The reduction of the RMS prediction error is on average 71% as compared to the results generated without the use of the Kalman filter.

3.2.3 Available power prediction

It is observed that the Dynamic Flow Predictor can predict turbine available power with an error of less than 15% over a time horizon of up to 5min. The available power P_{av} of a wind turbine (Göçmen et al., 2016) is calculated as

$$P_{av} = \frac{1}{2}\rho A_{rotor} u^3 c_{P,max} \tag{18}$$

where ρ is the air density, u the rotor effective wind speed and $c_{P,max}$ the maximum power coefficient of the turbine achievable at the present wind speed.

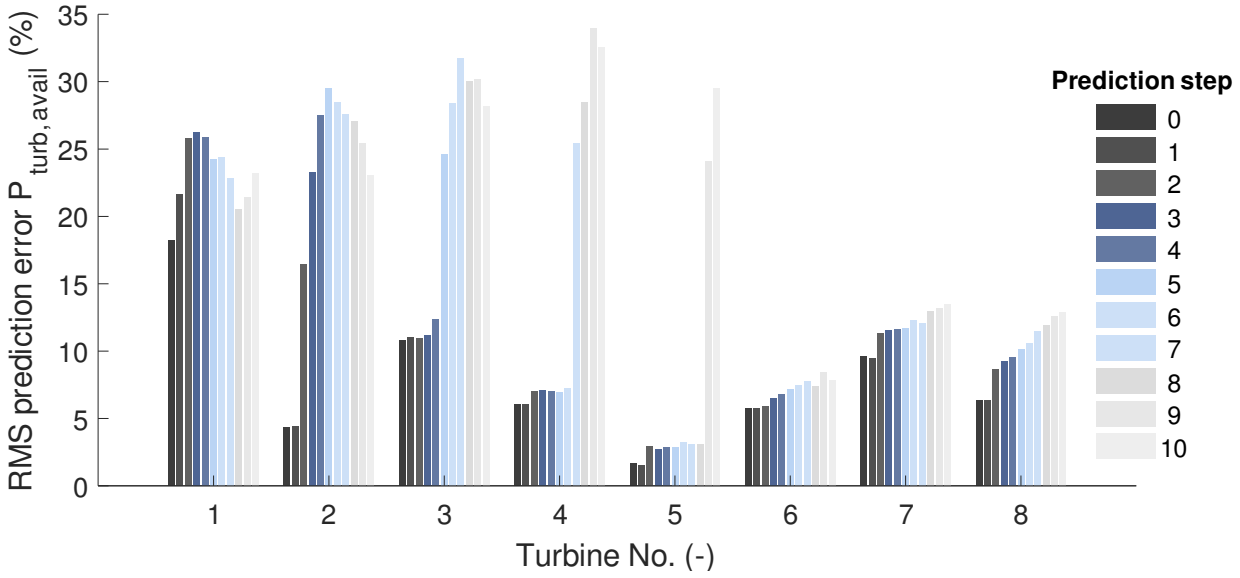

Figure 13. RMS error of 10-step ahead prediction of available power of turbines of eight turbine array.

Figure 13 shows the RMS error of the prediction of available power at the turbines of the eight turbine array. The available power prediction is calculated using the wind speed predictions obtained from the Dynamic Flow Predictor, including the Kalman filter. The observed pattern in the prediction error is the same as for the wind speed prediction accuracy statistics discussed with Figure 12. The available power predictions that are based on the model's internal delay states show prediction errors ranging from 1.5% to 14%. The larger error in available power prediction as compared to wind speed prediction is due to the error amplification in the calculation of power from wind speed.

3.3 Model application areas

The choice of a linear state space modelling approach enables the application of the Dynamic Flow Predictor in a wide range of control areas. Currently considered application areas of the Dynamic Flow Predictor are (i) wind farm control, (ii) turbine control and (iii) as virtual sensor. In the area of wind farm control, the model can be used in power reference following wind farm control. The model can predict the effect of turbine power set-points on turbine available power over the control horizon. Such predictions are particularly useful in model predictive power reference following wind farm control (Shapiro et al., 2018). In the second application area, turbine control, the model's predictions could be used as input to turbine controllers for an improved predictive control performance. In addition to direct use in control, the model's predictions can be used as a substitute of missing or temporarily unavailable turbine sensors at downstream turbines.

4 Conclusions

This work shows that the Dynamic Flow Predictor, a dynamic, linear, engineering model, can provide accurate estimates and predictions of wind turbine rotor effective wind speed and power in SimWindFarm. The Dynamic Flow Predictor can thus capture the dynamics of wind farm flow modelled by the higher fidelity model SimWindFarm. Wind speed is estimated with a RMS error ranging between 0.6% and 3.5%. Wind speed predictions can be provided with an error of less than 4% over a time horizon of 5min. Over the same 5min time horizon, turbine available power is predicted with an error of less than 15%. In the two turbine set-up the Dynamic Flow Predictor requires only 0.5% of the states of a comparable 2D dynamic CFD model. As a result, the Dynamic Flow Predictor is expected to be computationally less expensive than such CFD models. The choice of a linear state space modelling approach enables the Dynamic Flow Predictor's application in a wide range of control areas. Currently envisioned application areas are wind farm control, wind turbine control and as virtual wind turbine sensor.

Competing interests. There is no competing interests.

Acknowledgements. This work is funded by the CONCERT project, which is funded by Energinet.dk under the Public Service Obligation scheme (ForskEL 12396) with project partners Vattenfall R&D and Siemens Wind Power. Siemens Wind Power and Vattenfall R&D are gratefully acknowledged for their fruitful discussions.

References

Boersma, S., Gebraad, P., Vali, M., Doekemeijer, B., and van Wingerden, J.: A Control-oriented Dynamic Wind Farm Flow Model: "WFSim", Journal of Physics: Conference Series, 753, 032 005, 2016.

Boersma, S., Doekemeijer, B., Vali, M., Meyers, J., and Wingerden, J.-w. V.: A Control-oriented Dynamic Wind Farm Model : WFSim, Wind Energy Science, 3, 75, 2018.

Crespo, A. and Hernández, J.: Turbulence Characteristics in Wind-turbine Wakes, Journal of Wind Engineering and Industrial Aerodynamics, 61, 71–85, 1996.

Doekemeijer, B. M., Van Wingerden, J. W., Boersma, S., and Pao, L. Y.: Enhanced Kalman Filtering for a 2D CFD NS Wind Farm Flow Model, Journal of Physics: Conference Series, 753, https://doi.org/10.1088/1742-6596/753/5/052015, 2016.

Frandsen, S., Barthelmie, R., Pryor, S., Rathmann, O., Larsen, S., and Hojstrup, J.: Analytical Modelling of Wind Speed Deficit in Large Offshore Wind Farms, Wind Energy, 9, 39–53, 2006.

Gebraad, P. M. O. and van Wingerden, J.-W.: A Control-Oriented Dynamic Model for Wakes in Wind Plants, Journal of Physics: Conference Series, 524, 012 186, 2014.

Gebraad, P. M. O., Teeuwisse, F. W., van Wingerden, J. W., Fleming, P. A., Ruben, S. D., Marden, J. R., and Pao, L. Y.: Wind Plant Power Optimization Through Yaw Control using a Parametric Model for Wake Effects-a CFD Simulation Study, Wind Energy, 19, 95–114, 2016.

Göçmen, T., Giebel, G., Sørensen, P. E., and Poulsen, N. K.: Possible Power Estimation of Down-Regulated Offshore Wind Power Plants., Ph.D. thesis, 2016.

Grunnet, J., Soltani, M., and Knudsen, T.: Aeolus Toolbox for Dynamics Wind Farm Model, Simulation and Control, in: European Wind Energy Conference, p. 10, 2010.

Grunnet, J., Soltani, M., and Knudsen, T.: SimWindFarm Official Website, http://www.ict-aeolus.eu/SimWindFarm/index.html, 2016.

Jonkman, J., Butterfield, S., Musial, W., and Scott, G.: Definition of a 5-MW Reference Wind Turbine for Offshore System Development, in: NREL/TP-500-38060, 2009.

Jung, J. and Broadwater, R. P.: Current Status and Future Advances for Wind Speed and Power Forecasting, Renewable and Sustainable Energy Reviews, 31, 762–777, 2014.

Kalman, R. E. and Bucy, R. S.: New Results in Linear Filtering and Prediction Theory, Journal of Basic Engineering, 83, 95, 1961.

Kazda, J., Göçmen, T., Giebel, G., and Cutululis, N.: Possible Improvements for Present Wind Farm Models Used in Optimal Wind Farm Controllers, in: Wind Integration Workshop, 2016a.

Kazda, J., Gogmen, T., Giebel, G., Courtney, M., and Cutululis, N.: Framework of Multi-objective Wind Farm Controller Applicable to Real Wind Farms, in: WindEurope Summit 2016, 2016b.

Kazda, J., Merz, K., Tande, J. O., and Cutululis, N. A.: Mitigating Turbine Mechanical Loads Using Engineering Model Predictive Wind Farm Controller, in: IOP Conference Series - Journal of Physics - submitted, 2018.

Knudsen, T., Bak, T., and Soltani, M.: Prediction Models for Wind Speed at Turbine Locations in a Wind Farm, Wind Energy, 14, 877–894, 2011.

Machefaux, E., Larsen, G. C., Troldborg, N., Gaunaa, M., and Rettenmeier, A.: Empirical Modeling of Single-wake Advection and Expansion Using Full-scale Pulsed Lidar-based Measurements, Wind Energy, 18, 2085–2103, 2015.

Mikkelsen, T., Angelou, N., Hansen, K., Sjoholm, M., Harris, M., Slinger, C., Hadley, P., Scullion, R., Ellis, G., and Vives, G.: A Spinner-integrated Wind Lidar for Enhanced Wind Turbine Control, Wind Energy, 16, 625–643, 2013.

Pao, L. Y. and Johnson, K. E.: A Tutorial on the Dynamics and Control of Wind Turbines and Wind Farms, in: American Control Conference. ACC '09. IEEE, pp. 2076–2089, IEEE, 2009.

Riverso, S., Mancini, S., Sarzo, F., and Ferrari-Trecate, G.: Model Predictive Controllers for Reduction of Mechanical Fatigue in Wind Farms, IEEE Transactions on Control Systems Technology, 25, 535–549, 2017.

Schlipf, D., Schlipf, D. J., and Kühn, M.: Nonlinear Model Predictive Control of Wind Turbines Using LIDAR, Wind Energy, 16, 1107–1129, 2013.

Shapiro, C. R., Meyers, J., Meneveau, C., and Gayme, D. F.: Wind Farms Providing Secondary Frequency Regulation: Evaluating the Performance of Model-based Receding Horizon Control, pp. 11–24, 2018.

Soleimanzadeh, M., Wisniewski, R., and Brand, A.: State-space Representation of the Wind Flow Model in Wind Farms, Wind Energy, 17, 627–639, 2014.

Wang, J. and Hu, J.: A Robust Combination Approach for Short-term Wind Speed Forecasting and Analysis–Combination of the ARIMA (Autoregressive Integrated Moving Average), ELM (Extreme Learning Machine), SVM (Support Vector Machine) and LSSVM (Least Square SVM) Forecasts Using a GPR (Gaussian Process Regression) Model, Energy, 93, 41–56, 2015.